# A STUDY ON THE PROPULSIVE PERFORMANCE OF HI-FIN

Soo-Yeong Park, Bum-Woo Han and Bong-Jun Chang
Hyundai Maritime Research Institute, Hyundai Heavy Industries Co., LTD.
Seoul, 110-693, South Korea
sypark72@hhi.co.kr, sayyes@hhi.co.kr, bjchang@hhi.co.kr

**ABSTRACT:** With the increased interest in fuel saving technologies for ships, many kinds of energy saving devices (ESDs) have been developed and applied. Hi-Fin is a kind of energy saving device that has fin on the propeller boss cap which eliminates the hub vortex induced by propeller rotation as well as increases in propulsive efficiency. The aim of this study is to investigate the effects of Hi-Fin using computational fluid dynamics (CFD). To verify the numerical analysis results, propeller wake fields were measured by stereoscopic particle image velocimetry (SPIV) and self-propulsion test has been performed in Hyundai Maritime Research Institute (HMRI). The result shows a good agreement between calculations and measurements in model scale.

## INTRODUCTION

The requirement of higher fuel efficiency and the reduction of $CO_2$ emissions has been a key target in maritime industry since the International Maritime Organization (IMO) enacted the new regulations based on the Energy Efficiency Design Index (EEDI). The EEDI forced shipbuilders to make more energy efficient vessels, and in relation to this, much research and development of Energy Saving Devices (ESDs) have been conducted to increase propulsive efficiency. There are many types of ESDs such as Pre-Swirl Duct and Stator (PSD, PSS), Propeller Boss Cap Fin, Rudder Bulb, and so on. Among these ESDs, Propeller Boss Cap Fin is one of the most popular ESDs because it is relatively easy to manufacture and install, therefore, cost effective.

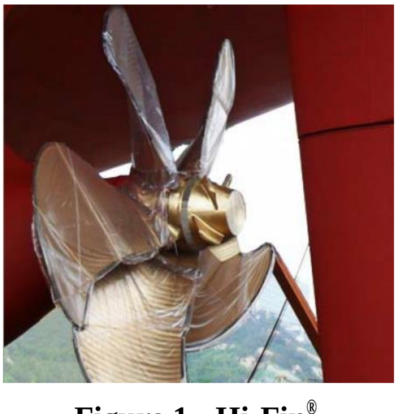

**Figure 1 - Hi-Fin®**

With regard to the propulsive efficiency of Propeller Boss Cap Fin, Ouchi et al. analyzed the features of Propeller Boss Cap Fin which improves propulsive efficiency by reducing hub vortex through flow visualization, propeller open water test and on ship scale test [1, 2]. Hansen et al. performed self-propulsion test with Propeller Boss Cap Fin and the result shows that propulsion efficiency gain in self-propulsion test was larger than the improvement in open water efficiency [3]. Lim et al. examined the design parameters of Propeller Boss Cap Fin via CFD analysis with propeller open water (POW) test and reported that the pitch and the chord to span ratio have the greatest effect on the propulsive efficiency [4]. Han el al. investigated the effect of Propeller Boss Cap Fin by analyzing wake field characteristics of a Propeller Boss Cap Fin with design parameter variations, paying particular attention to hub vortex dynamics [5].

Hyundai Heavy Industries (HHI) developed Hi-Fin which is a kind of fin with an end-plated on the propeller boss cap. The end-plate enables relatively small area of the fin to generate the similar performance as a conventional fin as found in the winglet of an airplane, and as a result, the length of the boss cap is shortened to increase applicability. Fig. 1 shows a Hi-Fin installed on a ship.

The purpose of the present study is to verify the propulsive performance of Hi-Fin. For this purpose, propeller open water analysis as well as self-propulsion computation with full geometry of hull, rudder and propeller is performed by CFD. Furthermore, the wake field characteristic of a propeller and Hi-Fin was investigated. For validation, the propeller wake field was measured by stereoscopic particle image velocimetry (SPIV) and self-propulsion tests were conducted at the HMRI (Hyundai Maritime Research Institute).

## DESCRIPTION OF NUMERICAL CALCULATION

### Propeller model

A drawing of propeller for container ships (KP505) shown in fig. 2 was used in the present study. The general information on the propeller is shown in table 1.

| | | | |
|---|---|---|---|
| Diameter | 270 mm | Expanded area ratio | 0.800 |
| Number of blade | 5 | Skew angle | 32.0 deg |
| Pitch ratio at 0.7R | 0.997 | Blade section | NACA66 |

**Table 1- Principal particulars of the propeller**

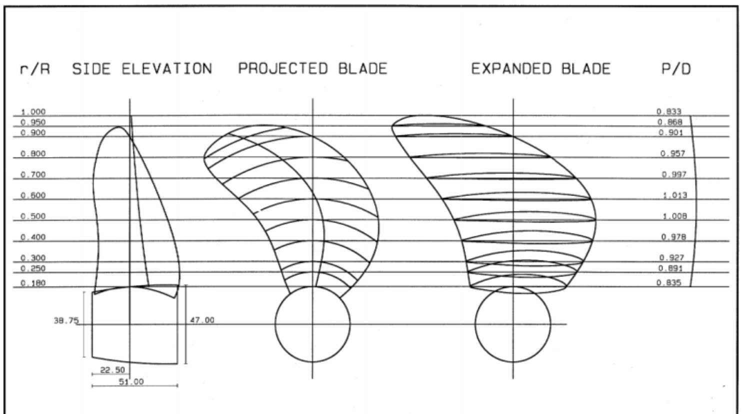


**Figure 2- Propeller drawing**

**Numerical calculation method for open water simulation and self-propulsion test**

Commercial CFD software STAR-CCM+ was used to carry out open water and self-propulsion simulation in model scale. The governing equations are the Reynolds Averaged Navier-Stokes equations. All the simulations were applied the *k-ω-SST* model for the turbulence model. For the propeller open water simulation, moving reference approach is applied because the inflow velocity is uniform. For the self-propulsion simulation, both steady state and unsteady calculations are considered. Firstly, Moving Reference Frame (MRF) is applied for the convergence and effective calculation time, and the unsteady simulation of the rotating propeller was resolved using a time-accurate sliding mesh method. In the self-propulsion analysis the main concern is the relative comparison between the cases with and without Hi-Fin, free surface is not considered to increase efficiency of calculation time. By using the skin friction correction taken from the model test, self-propulsion point is achieved by adjusting the propeller revolution rate.

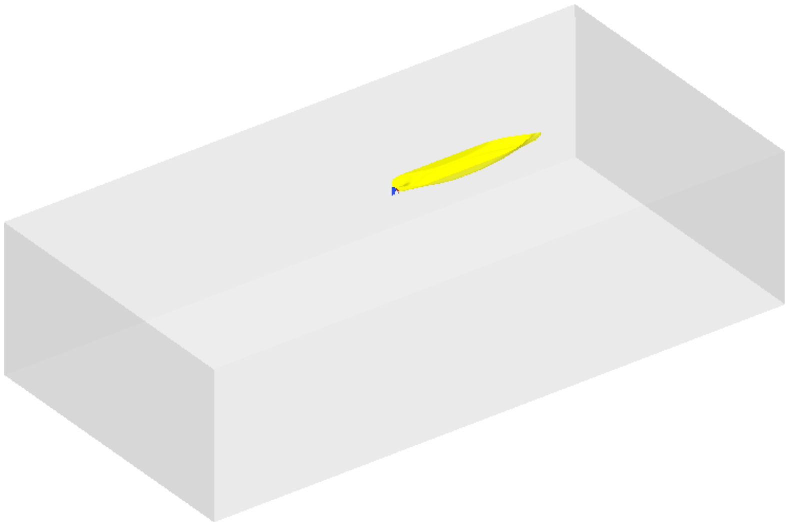

**Figure 3- Computation domain for self-propulsion analysis**

| Simulation | POW | Self-Propulsion |
|---|---|---|
| Governing equations | Reynolds-averaged Navier-Stokes (RANS) | |
| Turbulence model | *k-ω*-SST | |
| Scale | Model scale | |
| Propeller rotation | Rotating Reference Frame | Rotating Reference Frame and Rotation |
| Free surface | - | Not considered (symmetry boundary condition) |
| Multi-phase flow | - | Not considered |
| Prediction of self-propulsion point | - | 2 RPS and interpolation |

**Table 2- Description of the computational method**

Fig. 3 shows the computational domain for self-propulsion simulation. The computation domain was chosen to extend 1.0LBP from the bow to inlet, 1.5LBP length aft from the stern, 1.0LBP length in a width and depth direction. The trimmed mesh is applied in the main stationary fluid region and polyhedral mesh is applied in the rotating region. In order to resolve the boundary layer accurately, six layers of prismatic cells are applied along the hull, rudder, propeller, hub and Hi-Fin. Several volumetric controls were applied to capture the flow conditions that occur behind a hull. The computational mesh used for the self-propulsion simulation is approximately 7.4 million cells for the without Hi-Fin case and 7.8 million cells for the with Hi-Fin case. With such a mesh setting, the thickness of the first cell close to the hull and propeller, *Wall y+* values were achieved within 10 to 30 which can be regarded as sufficient for near wall treatment with the All *y+* wall treatment for the self-propulsion calculations. Table 2 lists the description of the computation method for propeller open water and self-propulsion simulation.

## DESIGN OF HI-FIN

As the first stage of the present study, a parameter study of Hi-Fin has been conducted to optimize the performance of Hi-Fin. Design parameters of Hi-Fin, such as fin area, pitch angle of fin and phase angle between propeller G.L. and fin C.L were selected and varied to control the fin loading. The fin area was varied by changing the fin height and length. Reference geometry of Hi-Fin used for the parameter study is listed in table 3. Pitch angle of reference Hi-Fin selected was 56˚, which is equal to propeller root pitch angle.

| Design parameter of Hi-Fin | Reference Hi-Fin |
|---|---|
| Fin length and height | 20.28mm |
| Pitch angle of fin | 56˚ |
| Phase angle between propeller G.L. and fin C.L. | 0˚ |

**Table 3- Reference geometry of Hi-Fin**

Fig. 4 shows parameter study result in self-propulsion condition. The power denotes a computed value of $2 \cdot \pi \cdot n \cdot Q$. The smaller power value means better propulsive performance because the ship can go forward with less power. From fig. 4 (a), it is seen that there seems to be an optimum fin length and height, except when the power increases. Pitch angle of fin, as shown in fig. 4 (b), the power tends to decrease as the pitch angle of fin decreases. The smallest power can be obtained at a pitch angle of 44.0˚. Judging from the pitch angle of fin variation results, higher propulsive efficiency can be obtained as the angle of attack between propeller root section and Hi-Fin decreases and there is a certain point that can maximize the performance of Hi-Fin. Phase angle between propeller G.L. and fin C.L. is varied between two blades of the propeller. The smallest power can be obtained at a phase angle of -12.0˚, however, difference between maximum and minimum power value is quite low. From the results, it can be deduced that phase angle difference between propeller G.L. and fin C.L. have a negligible effect on the propulsive performance.

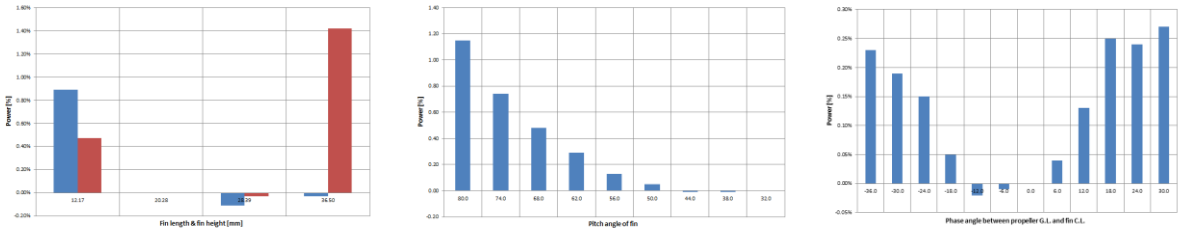

**(a) Fin length and fin height** **(b) Pitch angle of fin** **(c) Phase angle between propeller G.L. and fin C.L.**

**Figure 4- Parameter study**

## NUMERICAL ANALYSIS RESULTS AND VALIDATION BY EXPERIMENTS

Model propeller (KP505) and selected design of Hi-Fin after the design parameter study based on the numerical analysis are manufactured for the validation of computation results. Fig. 5 shows the geometry of the base case and Hi-Fin used for the validation.

**Figure 5- Hi-Fin model, left: Base case, right: Hi-Fin**

All the results were compared with the base case (w/o Fin) and Hi-Fin installed condition.

### Open water performance

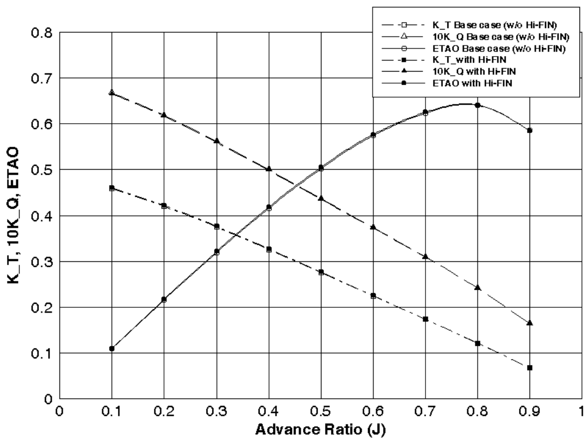


**Figure 6- Propeller open water performance**

In order to understand open water characteristics of Hi-Fin, open water analysis has been performed before proceeding to a self-propulsion simulation. In the POW simulation, all the simulation has been carried out with a constant propeller revolution rate of 9 per second. Fig. 6 shows the numerical calculation results of the open water performance for the propeller with base case and it was compared to the case for the propeller with Hi-Fin. The results show that the Hi-Fin has an effect on the total propeller open water efficiency increase around 0.7% in J under 0.5 and the maximum efficiency was 0.8% found at J=0.3. Total efficiency gain is decreased as the advance ratio is increased.

**Influence of Hi-Fin on self-propulsion condition**

Fig. 7 shows the pressure distribution on propeller surface with base case and Hi-Fin in self-propulsion condition. It is seen that there is much negative pressure region at the rear part of hub cap in base case. Whereas, strong negative pressure region is significantly disappeared in the Hi-Fin case. From the results, it is expected that hub vortex will be eliminated due to pressure increase.

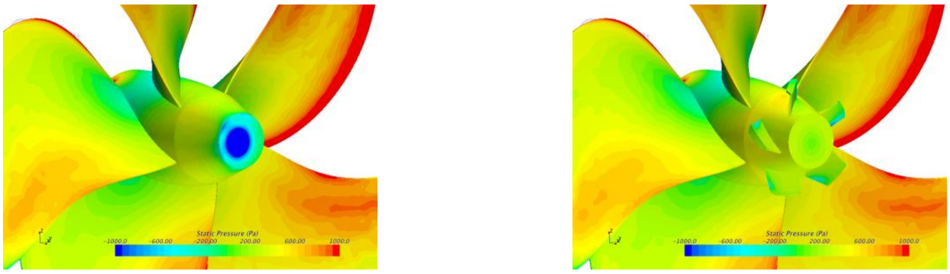

**(a) Base case** **(b) Hi-Fin**

**Figure 7- Comparison of pressure distribution with base case and Hi-Fin**

Figs. 8~15 show the wake fields of CFD analysis and SPIV measurement results behind the working propeller in base case and Hi-Fin installed condition. Although there is wake distribution discrepancy between the computation and experiment results, as shown in figs. 8, 9, 12, 13 (c), wake distribution difference between two techniques are not so large and overall flow characteristics are well captured. Focusing on the propeller hub, strong rotational flow can be seen with the base case hub cap condition in figs. 8 (a), (b). This tendency still exists in the downstream of the propeller even though the swirl flow is relatively weakened as shown in figs. 9 (a), (b). The effect of Hi-Fin is more clearly seen in vorticity contours. Comparing the vorticity contours downstream of propeller plane (x/R=0.6) as shown in figs. 10 (a), (b) and figs. 14 (a), (b), it is seen that strong vorticity magnitudes are significantly reduced after installation of Hi-Fin. Meanwhile, vorticity contour discrepancies between computation and experiment results shown in figs. 11 (a), (b) and figs. 15 (a), (b) are mainly due to the numerical dissipation of RANS simulation with $k$-$\omega$-SST turbulence model.

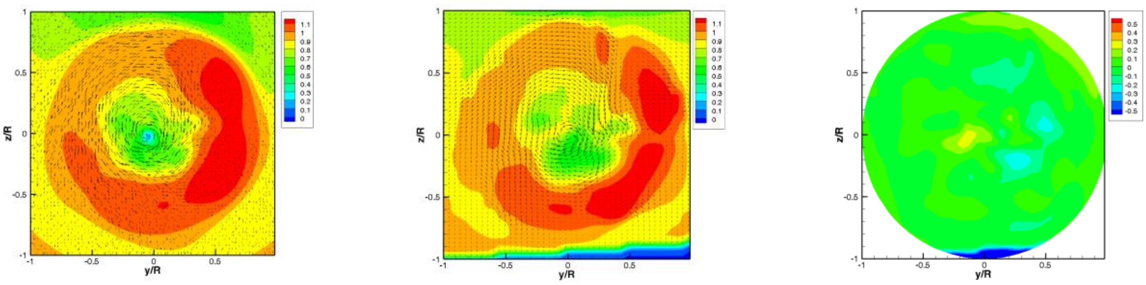

**(a) Axial velocity contours using CFD** **(b) Axial velocity contours using SPIV** **(c) Contours of axial velocity difference between CFD and SPIV**

**Figure 8- Axial velocity contours downstream of propeller plane(x/R=0.6) with base case**

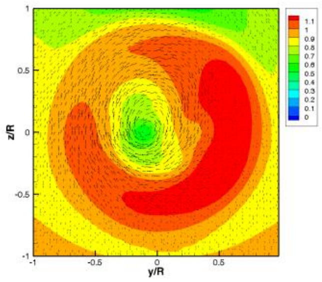

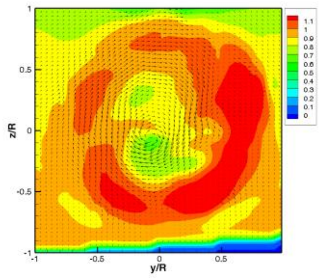

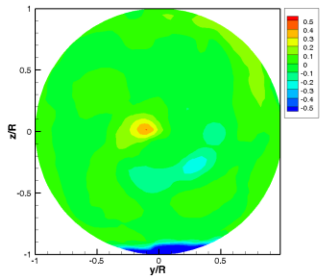

(a) Axial velocity contours using CFD

(b) Axial velocity contours using SPIV

(c) Contours of axial velocity difference between CFD and SPIV

**Figure 9- Axial velocity contours downstream of propeller plane(x/R=1.0) with base case**

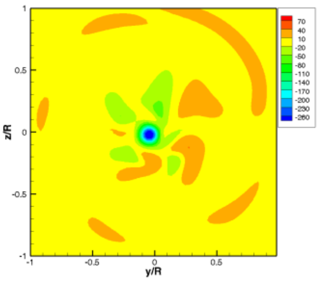

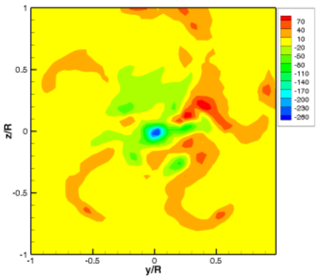

(a) Vorticity contours using CFD

(b) Vorticity contours using SPIV

**Figure 10- Vorticity contours downstream of propeller plane(x/R=0.6) with base case**

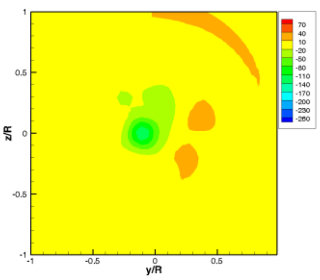

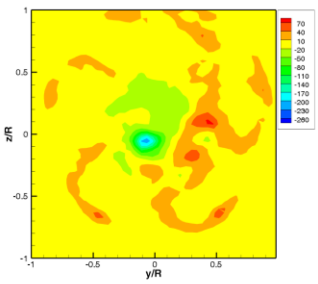

(a) Vorticity contours using CFD

(b) Vorticity contours using SPIV

**Figure 11- Vorticity contours downstream of propeller plane(x/R=1.0) with base case**

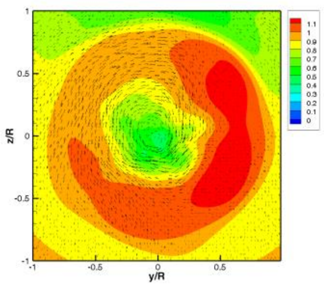

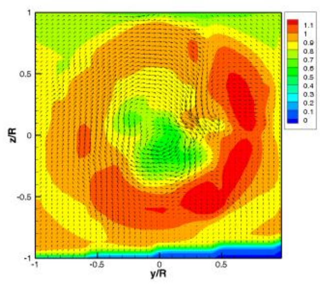

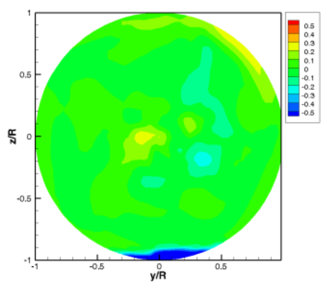

(a) Axial velocity contours using CFD

(b) Axial velocity contours using SPIV

(c) Contours of axial velocity difference between CFD and SPIV

**Figure 12- Axial velocity contours downstream of propeller plane(x/R=0.6) with Hi-Fin**

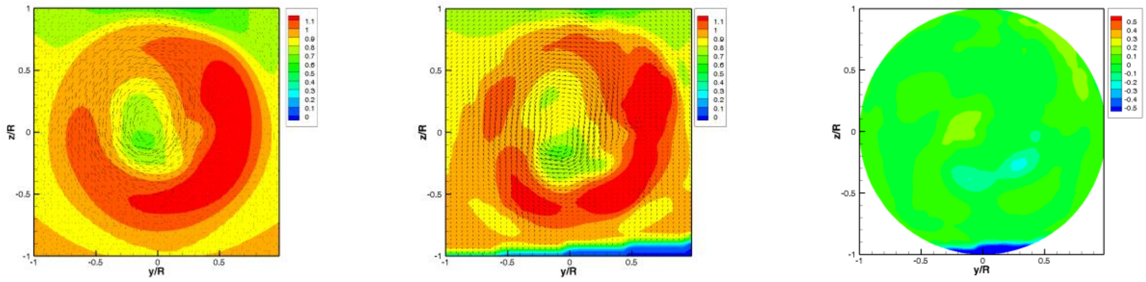

**(a) Axial velocity contours using CFD** **(b) Axial velocity contours using SPIV** **(c) Contours of axial velocity difference between CFD and SPIV**

**Figure 13- Axial velocity contours downstream of propeller plane(x/R=1.0) with Hi-Fin**

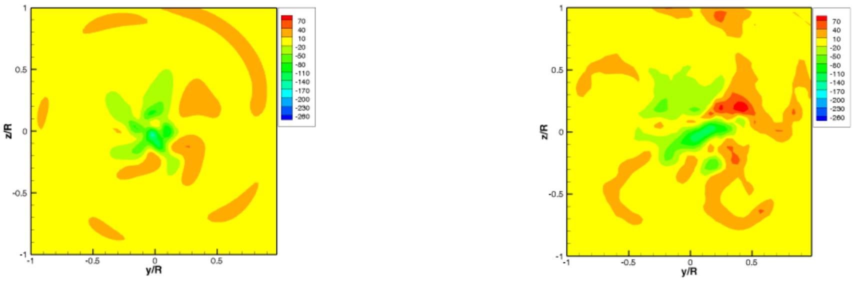

**(a) Vorticity contours using CFD** **(b) Vorticity contours using SPIV**

**Figure 14- Vorticity contours downstream of propeller plane(x/R=0.6) with Hi-Fin**

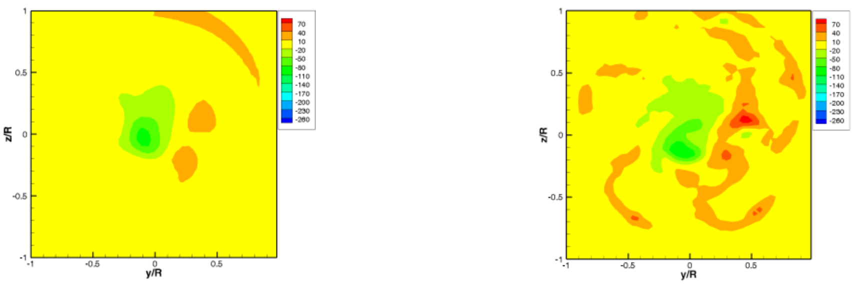

**(a) Vorticity contours using CFD** **(b) Vorticity contours using SPIV**

**Figure 15- Vorticity contours downstream of propeller plane(x/R=1.0) with Hi-Fin**

Fig. 16 shows the axial and tangential velocity field of CFD analysis and SPIV measurement results in self-propulsion condition. Each velocity component is plotted as a non-dimensional velocity. Except the behind propeller at shaft center of CFD analysis results, the velocity behind the Hi-Fin in the axial velocity downstream of propeller plane (x/R=0.6) was lower than that behind base case. However, axial velocity component accelerated rapidly in the downstream of the propeller hub (x/R=1.0). It is clearly seen that the axial velocity behind the Hi-Fin case is greater than that of the behind the base case in CFD analysis results. On the other hand, axial velocity downstream of propeller plane (x/R=1.0) shows the difference tendency between CFD analysis and SPIV measurement results. The larger test uncertainty in this case may have caused the greater axial velocity field measurements. From the axial velocity field calculation results, it can be deduced that the Hi-Fin generates the thrust by accelerating the flow in the downstream, although the effect is minor. Comparing the tangential velocity, it is clearly seen that tangential velocity is significantly reduced by fitting the Hi-Fin. From the results, one can expect that the torque will be reduced after installation of Hi-Fin by minimizing the strong swirl flow.

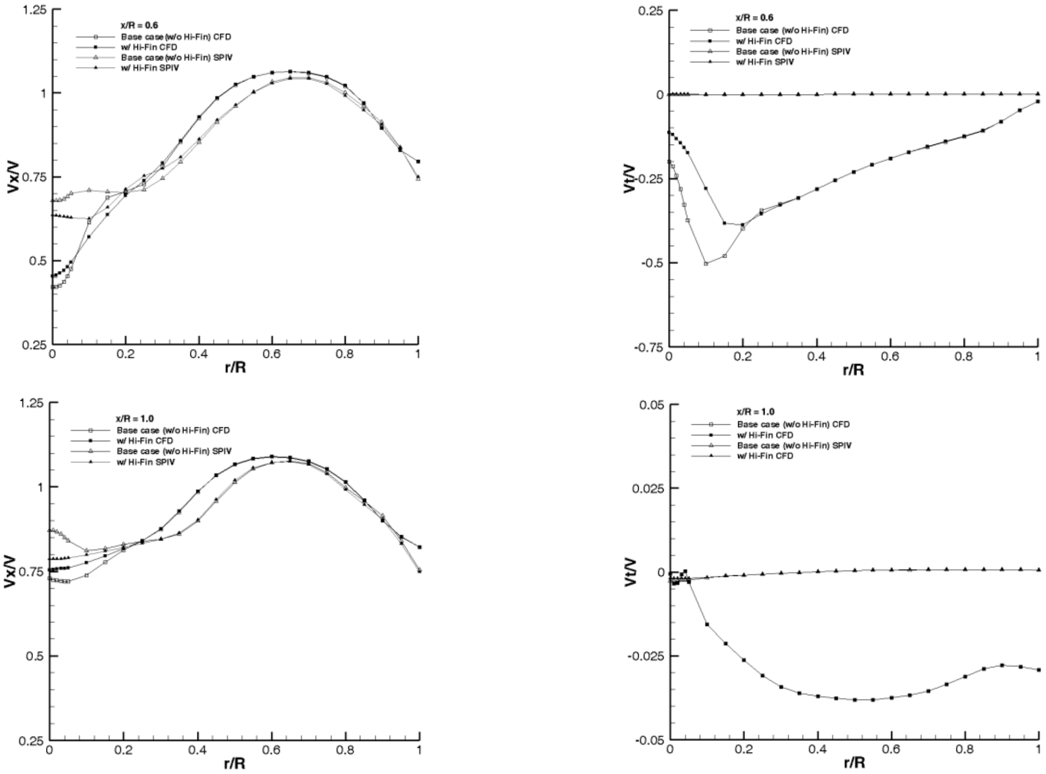


**Figure 16- Axial, Tangential flow velocities behind propeller**

<table>
<tr><td colspan="2" rowspan="2">Content</td><td colspan="3">CAL</td><td colspan="2">EXP</td></tr>
<tr><td>Base Case</td><td colspan="2">w/ Hi-Fin</td><td>Base Case</td><td>w/ Hi-Fin</td></tr>
<tr><td colspan="2">RPS</td><td>6.954<br>(+1.5%)</td><td colspan="2">6.932<br>(+1.6%)</td><td>6.849</td><td>6.826</td></tr>
<tr><td rowspan="2">Thrust<br>[N]</td><td>Propeller</td><td>48.596<br>(+0.2%)</td><td>48.112</td><td rowspan="2">(+0.4%)</td><td>48.519</td><td rowspan="2">48.023</td></tr>
<tr><td>Hi-Fin</td><td>-</td><td>0.124</td><td>-</td></tr>
<tr><td rowspan="2">Torque<br>[N·m]</td><td>Propeller</td><td>2.2193<br>(+4.4%)</td><td>2.1914</td><td rowspan="2">(+4.6%)</td><td>2.1257</td><td rowspan="2">2.0896</td></tr>
<tr><td>Hi-Fin</td><td>-</td><td>-0.0052</td><td>-</td></tr>
<tr><td colspan="2">Power [W]</td><td>96.967<br>(+6.0%)</td><td colspan="2">95.211<br>(+6.2%)</td><td>91.476</td><td>89.621</td></tr>
<tr><td colspan="2">Power reduction<br>by fitting Hi-Fin [%]</td><td colspan="3">-1.81%</td><td colspan="2">-2.03%</td></tr>
</table>

**Table 4- Comparison of self-propulsion performance between base case and Hi-Fin case**

In addition, self-propulsion tests with base case and Hi-Fin fitted case were also conducted for the validation. The results of calculation and experiment are summarized in table 4. Based on the calculation results, it seems that Hi-Fin itself produces thrust, however, propeller thrust is decreased due to the installation of Hi-Fin, and as a result, the total thrust is slightly reduced in Hi-Fin case. On the other hand, installation of Hi-Fin has greatly contributed to total torque decrease than total thrust reduction. Consequently, power is reduced in Hi-Fin case in comparison with the base case mainly due to the decrease in net torque. Propeller revolution rate decrease due to Hi-Fin also affected decrease in power. With the installation of Hi-Fin, power is reduced about 1.8% and 2.0% in calculation and experiment, respectively.

## CONCLUSION

This paper examined a propulsive performance of Hi-Fin by CFD and the results were compared with the model test results. Wake field measurements behind the propeller using SPIV system and self-propulsion tests have been performed to verify the validity of the computation results.

- A parameter study of Hi-Fin has been performed and the results showed that the most important factor that effects the performance was the fin length, chord, and pitch angle of the fin.
- According to the wake field behind the propeller on both CFD analysis and SPIV measurement results, the rotational flow and the magnitude of vorticity are reduced after installation of Hi-Fin.
- The self-propulsion test results showed that about 2.0% of power was reduced by fitting Hi-Fin. Although total thrust is reduced, a significant reduction of total torque improved the propulsive performance when fitted Hi-Fin.

As a future plan, the authors will continue to study about the performance of Hi-Fin in ship scale self-propulsion condition considering hull, rudder interaction.

## REFERENCES

1. Ouchi, K., Ogura, M., Kono, Y., Orito, H., Siotsu, T., Tamashima, M. and Koizuka, H. (1988) A research and development of PBCF (Propeller Boss Cap Fins)-improvement of flow from propeller boss, Journal of the Society of Naval Architecture of Japan, 163, 66-78.

2. Ouchi, K., Tamashima, M., Kawasaki, T. and Koizuka, H. (1989) A Research and development of PBCF (Propeller Boss Cap Fins): 2nd report: study on propeller slipstream and actual ship performance, Journal of the Society of Naval Architecture of Japan, 165, 43-53.

3. Hansen, H.R., Dinham-Peren, T. and Nojiri, T. (2011), Model and full sale evaluation of a ‘propeller boss cap fins’ device fitted to an Aframax tanker, International Symposium on Marine Propulsors, Hamburg, Germany, 186-196.

4. S.S. Lim, T.W. Kim, D.M. Lee, C.G. Kang and S.Y. Kim (2014) Parametric study of propeller boss cap fins for container ships, International Journal of Naval Architecture and Ocean Engineering, Vol. 6, 187-205.

5. B.W. Han, J.H. Seo, S.J. Lee and S.H. Rhee (2016) Parametric study on hub vortex reducing effects of Propeller Boss Cap Fins by force and wake field measurements, International Symposium on Transport Phenomena and Dynamics of Rotating Machinery.